

Broad-band spectral changes of the microquasars Cygnus X-1 and SWIFT J1753.5–0127

M. Cadolle Bel*

SAP/CEA-Saclay & AIM, Gif-sur-Yvette, France & ESAC, Madrid, Spain

E-mail: mcadolle@cea.fr

M. Ribó

Universitat de Barcelona, Spain

J. Rodriguez

SAP/CEA-Saclay & AIM, Gif-sur-Yvette, France

S. Chaty

SAP/CEA-Saclay & AIM, Gif-sur-Yvette, France

S. Corbel

SAP/CEA-Saclay & AIM, Gif-sur-Yvette, France

A. Goldwurm

SAP/CEA-Saclay & APC, Gif-sur-Yvette, France

We report high-energy results obtained with *INTEGRAL* and *Rossi-XTE* on two microquasars: the persistent high-mass system Cygnus X-1 and the transient low-mass binary SWIFT J1753.5-0127. *INTEGRAL* observed Cygnus X-1 from 2002 to 2004: the spectral (5–1000 keV) properties of the source, seen at least in three distinct spectral states, show disc and corona changes. In 2003 June, a high-energy tail at several hundred keV in excess of the thermal Comptonization model was observed, suggesting the presence of an additional non-thermal component. At that time, we detected an unusual correlation between radio data and high-energy hardness. We also report and compare the results obtained with simultaneous observations of the transient source SWIFT J1753.5-0127 performed with *Rossi-XTE*, *INTEGRAL*, VLA, REM and NTT on 2005 August 10–12 near its hard X-ray outburst. Broad-band spectra and fast time-variability properties are derived on this source (probably located in the galactic halo) together with radio, IR and optical data. We build a spectral energy distribution of the source and derive interesting multiwavelength constraints. Significantly detected up to 600 keV in a typical Low/Hard State, the transient does not seem to follow the usual radio/X-ray correlation.

VI Microquasar Workshop: Microquasars and Beyond

September 18-22 2006

Società del Casino, Como, Italy

*Speaker.

1. Introduction

Galactic Black Hole (BH) X-ray binary systems display high-energy emissions characterized by spectral and flux variabilities (from milliseconds to months). These systems are found in several spectral states (see definitions in Homan & Belloni 2005) giving us the possibility to study the physical properties of emitting regions (disc, corona, jets) and their evolutions. Soft and hard components (and reflection) are coupled to various properties of variabilities in the power spectrum (e.g., Belloni 2005) and in the radio (e.g., Corbel et al. 2003). A part from the Low/Hard States (LHS) and the High/Soft States (HSS) other ones have been identified characterized either by a greater luminosity than in the HSS or by variability and X-ray spectral properties mostly intermediate between the LHS and the HSS: the Hard and Soft Intermediate States (HIMS and SIMS).

Cygnus X-1 is one of the first X-ray binaries detected and has been extensively observed. Among the brightest X-ray sources of the sky, it is very variable on different time scales and a relativistic jet has been detected (Stirling et al. 2001). Located at 2.4 ± 0.5 kpc, the source accretes by strong stellar wind from a giant companion. Cygnus X-1 spends most of its time (70%) in the LHS. During the SIMS of 1996 June, in addition to the dominant black body component and the hard component, a high-energy tail extending up to 10 MeV was discovered (McConnell et al. 2002).

On the other hand, the study of Transient Sources (TS) which tend to evolve into the LHS in the late stages of an outburst (e.g., Cadolle Bel et al. 2004) may reveal important clues on its mechanisms and relation with the accretion rate (e.g., Homan et al. 2001; Rodriguez et al. 2003). The TS SWIFT J1753.5–0127 was discovered in hard X rays with the *Swift*/Burst Alert Telescope (BAT) on 2005 May 30 (Palmer et al. 2005). The *Swift*/X-ray Telescope (XRT) observation revealed a variable source; the source was also clearly detected in UV with the UV/optical Telescope (Still et al. 2005). On the ground, the optical MDM 2.4 m telescope revealed a new star within the *Swift* error circle (Halpern et al. 2005). At the beginning of July, Fender et al. (2005) reported with MERLIN a probable point-like radio counterpart (consistent with a compact jet). In X rays, the 1.2–12 keV source flux increased to the maximum value of ~ 200 mCrab in few days and started to decay slowly. The hard power law spectrum observed with the *Swift*/XRT (Morris et al. 2005) and the 0.6 Hz QPO detected in pointed *RXTE* observations (Morgan et al. 2005) are characteristic of the LHS as also reported later by Miller et al. (2006).

We report exciting results collected on Cygnus X-1 over two years with *INTEGRAL* (e.g., Cadolle Bel et al. 2006a, hereafter CB06a; Malzac et al. 2006). In parallel, we also report the results of our triggered Target of Opportunity (ToO) campaign for TS in the galactic halo (August 10–12) on SWIFT J1753.5–0127. Preliminary results reported in Cadolle Bel et al. (2005) showed that the TS was then still in a LHS. Thanks to a large multi-wavelength program we could also trigger simultaneously optical, infrared and radio ToOs and we added *RXTE* data in our analysis as explained in Cadolle Bel et al. 2006b (hereafter CB06b).

2. Observations and data reduction

2.1 Cygnus X-1

The periods of our *INTEGRAL* observations (epochs 1 to 4) are indicated on Fig. 1 (left) on

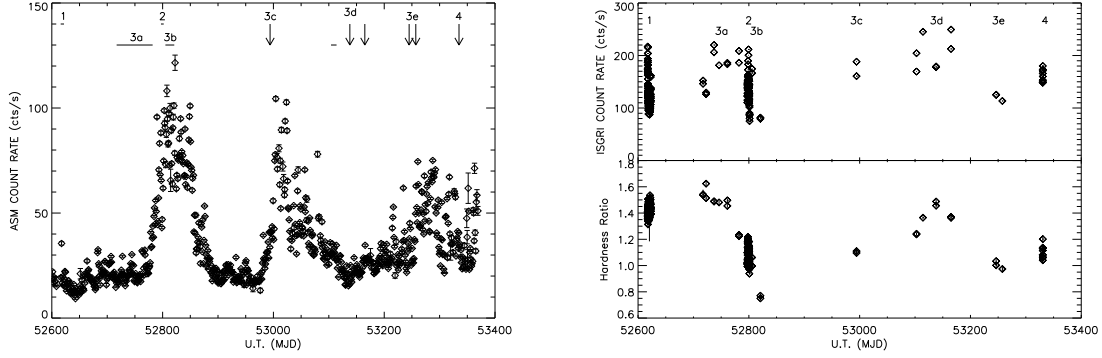


Figure 1: *Left:* *RXTE*/ASM daily average (1.2–12 keV) LC of Cygnus X-1 from 2002 November to 2004 November with the period of our *INTEGRAL* observations (see text and Table 1 for epoch definitions). *Right:* The 20–200 keV IBIS/ISGRI LC of Cygnus X-1 (top) and hardness ratio (bottom) between the 40–100 keV and 20–30 keV energy bands.

the *RXTE*/ASM Light Curve (LC). To discuss the time evolution of the source, IBIS/ISGRI LC and Hardness Ratios (HR) obtained over two years are reported in Fig. 1 (right). Epoch 1 (2002 December 9–11) includes part of the PV-Phase observations of Cygnus X-1. Epoch 2 corresponds to an Open Time observation performed on 2003 June 7–11 while epochs 3 and 4 refer respectively to the set of Cygnus X-1 observations during the GPS and the 2004 November calibrations.

2.2 SWIFT J1753.5-0127

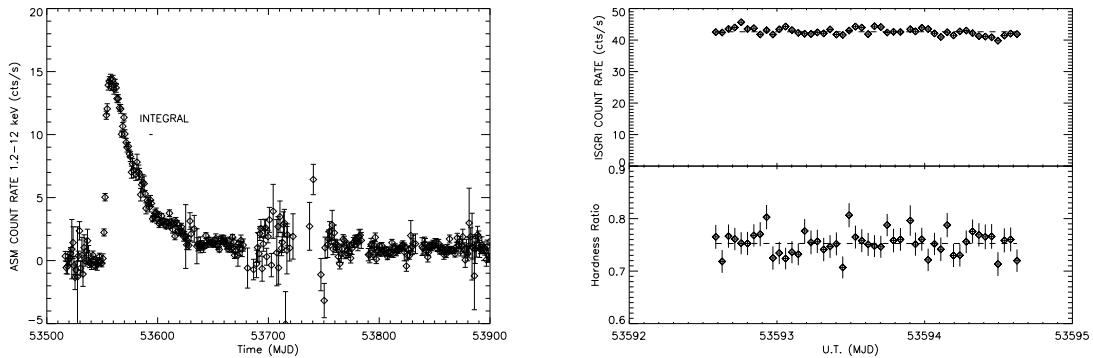


Figure 2: *Left:* *RXTE*/ASM daily average (1.2–12 keV) LC of SWIFT J1753.5–0127 from 2005 mid-May up to 2006 mid-June with our *INTEGRAL* ToO indicated. *Right:* The 20–320 keV IBIS/ISGRI LC of SWIFT J1753.5–0127 (top) and corresponding HR (bottom) between the 40–80 and 20–40 keV energy bands (errors at the 90% confidence level).

The journal of our simultaneous multiwavelength observations to our *INTEGRAL* ToO is given in CB06b in which we also detail our analysis procedures. Fig. 2 (left) plots the 1.2–12 keV *RXTE*/ASM daily average LC of SWIFT J1753.5–0127 since the discovery of the TS up to 2006 June 15 while Fig. 2 (right) shows the IBIS/ISGRI LC and HR during our multiwavelength ToO. Besides on 2005 August 11 (around UT 02) we also obtained optical photometry in *B*, *V* *R* and

I bands with the spectro-imager EMMI (NTT) and we observed SWIFT J1753.5–0127 with the NRAO VLA at 1.4, 4.9, 8.5 and 15 GHz on 2005 August 11 (average MJD 53593.28) with the VLA.

3. Spectral results on Cygnus X-1

As shown in Fig. 1 (left), during the epoch 2 *INTEGRAL* observations, the 1.5–12 keV ASM average count rate of Cygnus X-1 (~ 1.3 Crab) was larger than during epoch 1 (~ 290 mCrab) by a factor of 4.5. The derived IBIS/ISGRI 20–200 keV LC and HR of Cygnus X-1 are shown in Fig. 1 (right, epochs 1 to 4). From epoch 1 to epoch 2, while the ASM average count rate increased, the 20–200 keV IBIS/ISGRI one decreased from ~ 910 to ~ 670 mCrab. This probably indicates a state transition as also suggested by the decrease in the IBIS HR (the source softens). Similar transitions, with a change in the ASM LC and an evolving IBIS HR, occurred again during epoch 3 and epoch 4. Table 1 gives all the best-fit parameters of Cygnus X-1 with a model involving Comptonization (Titarchuk 1994), reflection (Magdziarz & Zdziarski 1995) and when needed a multicolor black body disc (Mitsuda et al. 1984) and Fe line components (modelling approach described in CB06a).

Table 1: Best-fit parameters of Cygnus X-1 for the current thermal model in the several observation epochs. Model in XSPEC notations: CONSTANT*WABS*(DISKBB+GAUSSIAN+REFLECT*COMPTT) with $N_{\text{H}}=6 \times 10^{21} \text{cm}^{-2}$ and kT_0 value tied to disc kT_{in} . Errors are at 90% confidence level ($\Delta\chi^2 = 2.7$).

Epochs, dates (MJD)	K^a	kT_{in} or kT_0 (keV)	kT_{e} (keV)	τ	E_{Fe} line (keV)	$\Omega/2\pi^b$	χ_{red}^2 (dof)
1, 52617-620	-	0.20 (frozen)	67_{-6}^{+8}	$1.98_{-0.23}^{+0.21}$	-	$0.25_{-0.04}^{+0.03}$	1.45 (230)
2, 52797-801	250_{-59}^{+89}	1.16 ± 0.07	100_{-17}^{+29}	$0.98_{-0.28}^{+0.25}$	$7.07_{-0.11}^{+0.12}$	$0.57_{-0.06}^{+0.09}$	1.69 (236)
3a, 52710-780	-	0.20 (frozen)	68_{-12}^{+22}	$2.08_{-0.84}^{+0.51}$	6.48 ± 0.13	$0.32_{-0.07}^{+0.05}$	1.07 (190)
3b, 52801-825	312_{-24}^{+25}	1.15 ± 0.03	93 ± 42	$0.80_{-0.40}^{+0.86}$	6.40 ± 0.73	$0.58_{-0.18}^{+0.20}$	0.93 (190)
3c, 52990	361_{-67}^{+61}	0.99 ± 0.08	58_{-15}^{+54}	$1.60_{-0.80}^{+0.64}$	6.96 ± 0.19	$0.23_{-0.09}^{+0.17}$	0.99 (190)
3d, 53101-165	-	0.20 (frozen)	56_{-7}^{+12}	$2.28_{-0.41}^{+0.30}$	6.11 ± 0.26	0.27 ± 0.06	0.81 (190)
3e, 53240-260	132 ± 10	1.39 ± 0.77	48_{-6}^{+20}	$1.85_{-0.07}^{+0.40}$	6.49 ± 0.38	$0.49_{-0.32}^{+0.37}$	1.56 (190)
4, 53335	232_{-32}^{+21}	1.16 (frozen)	128_{-63}^{+84}	$0.74_{-0.38}^{+0.88}$	$7.78_{-0.42}^{+0.44}$	$0.47_{-0.14}^{+0.18}$	0.97 (221)

Notes:

a) Disc normalization $K = (R/D)^2 \cos \theta$ (R : inner disc radius in units of km; D : distance to the source in units of 10 kpc; $\theta = 45^\circ$).

b) Solid angle of the reflection component.

3.1 The Low/Hard State spectrum

Fig. 3 (left) shows the resultant $EF(E)$ spectrum and its best-fit with the JEM-X, IBIS and SPI data during epoch 1. The best-fit model is reported in Table 1. The disc black body is very

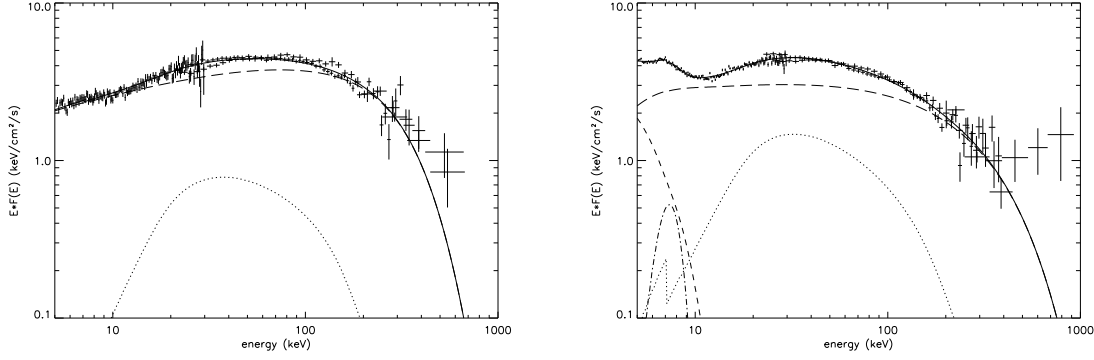


Figure 3: *Left:* Epoch 1 unabsorbed $EF(E)$ spectrum of Cygnus X-1 along with the best-fit model described in Table 1 with the JEM-X, SPI and IBIS (ISGRI and PICsIT) data. *Right:* The same for epoch 2. *Dotted:* reflection. *Long dashes:* Comptonization. *Dashed:* disc. *Dotted-dashed:* gaussian line. *Thick:* total model.

weak or below the energy range of JEM-X. While the 20–100 keV luminosity is $6.5 \times 10^{36} \text{ erg s}^{-1}$ (at 2.4 kpc), the bolometric (extrapolated from 0.01 keV to 10 MeV) luminosity has the value of $2.2 \times 10^{37} \text{ erg s}^{-1}$. These parameters are consistent with those found in BH binaries in the LHS as fully discussed in CB06a.

3.2 Transitions to Soft Intermediate States (SIMS)

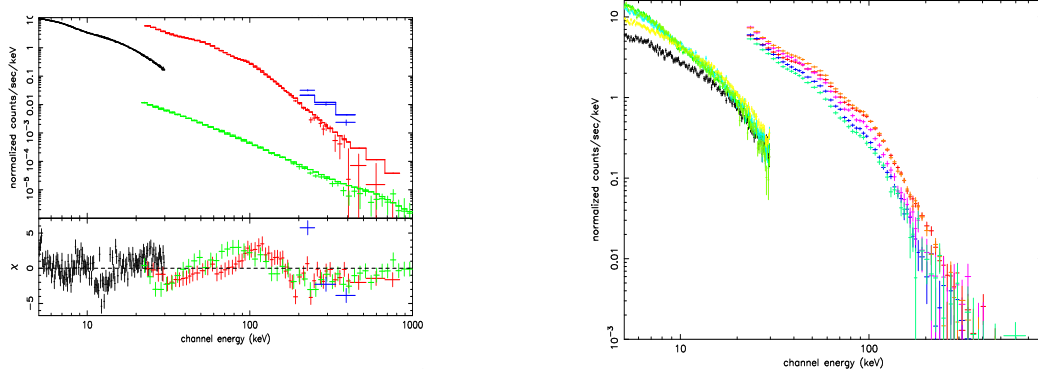


Figure 4: *Left:* Spectra of Cygnus X-1 during epoch 2 with JEM-X (black), SPI (green) and IBIS (ISGRI: red; PICsIT: blue) along with the best-fit hybrid model of Coppi (1999) including a non-thermal distribution for corona particles. Residuals in σ units are also shown. *Right:* Spectra of Cygnus X-1 during epoch 3 with JEM-X and IBIS/ISGRI along with the best-fit hybrid model (see Table 1).

Fig. 3 (right) shows the resultant $EF(E)$ spectrum and its best-fit with the JEM-X, IBIS and SPI data during epoch 2. Table 1 summarizes the best-fit parameters and the χ_{red}^2 obtained from 5 keV up to 1 MeV. We get a plasma temperature and an optical depth respectively higher and lower than in epoch 1. The disc accounts for 26 % of the total luminosity and the reflection is higher in epoch 2 than in epoch 1. Considering the behaviour of the ASM, IBIS LC and HR (Fig.1), the relative softness of the spectrum and the presence of a relatively strong hard energy emission, it

appears that during the 2003 June observations Cygnus X-1 was in the SIMS. This is also confirmed by radio observations of Malzac et al. (2006) who suggested that the fluctuations of the radio luminosity were associated with a pivoting of the high-energy spectrum and that the source did not display the usual radio/X-ray correlation. The derived thermal Comptonization parameters are consistent with those found in BH binaries in SIMS (McClintock & Remillard 2006).

As one can be seen in Fig. 3 (right), an excess with respect to the Comptonized spectrum above 400 keV is observed in the SPI data (not present in epoch 1 and not due to instrumental effects). Consequently we fitted the data with the hybrid model of Coppi (1999) coupled to the usual disc and Fe line components. Fig.4 (left) shows the resultant count spectrum obtained in epoch 2 with this model: with a $\chi^2_{\text{red}} = 1.55$ (232 dof), clearly better than the current epoch 2 thermal model, the derived thermal values of τ , $\Omega/2\pi$, E_{Fe} centroid and EW match, within the uncertainties, the parameters obtained in Table 1. The value of kT_e (42 keV) decreases from the pure thermal model as expected. The non-thermal electron power represents $\sim 16\%$ of the total power supplied to the electrons in the corona. The inferred bolometric luminosity is 3.3×10^{37} erg s $^{-1}$. Similar spectral transitions seem to occur later: epochs 3 *a* to *e*) are close pointings which occur (see Fig. 1) in different regimes of ASM count rate and of average IBIS HR. The best-fit spectral results (Table 1) we obtained on JEM-X and IBIS/ISGRI data (Fig. 4, right) indicate that, during sub-groups 3*a* and *d*, Cygnus X-1 was in a LHS (as in epoch 1) while, in sub-groups 3*b*, *c* and *e* and in epoch 4, the source was in a softer state (HSS or SIMS) as explained in CB06a.

4. Multiwavelength results on SWIFT J1753.5-0127

4.1 Light curves and timing variabilities

From the end of 2005 May up to July 9, the ASM average count rate increased (Fig. 2, left): its flux reached the maximum value of ~ 200 mCrab (MJD 53560) and then decreased to ~ 14 mCrab (MJD 53650). The characteristic decay time we derived (37.0 ± 0.2 days) is compatible with the usual behaviour of TS in outburst (Tanaka & Shibazaki, 1996; Chen et al. 1997) like, e.g., XTE J1720–318 (Cadolle Bel et al. 2004). During our *INTEGRAL* ToO the IBIS/ISGRI count rate was almost constant at 43 cts s $^{-1}$ (~ 205 mCrab) between MJD 53592–53594.4 (Fig. 2, right, top) with a constant HR (~ 0.75).

We produced a Power Density Spectrum (PDS) with the PCA data : the continuum is well represented by the sum of two zero-centered broad Lorentzians while an additional third Lorentzian is needed to account for a QPO around 0.24 Hz. This value is lower than the 0.6 Hz QPO reported after the peak of the outburst: this trend is sometimes observed in other BHCs and has been associated to the recession of the accretion disc (Kalemci et al. 2002; Rodriguez et al. 2004; Belloni et al. 2005). However, we can not exclude another interpretation for the QPO based on the pulsation modes of the corona (Shaposhnikov & Titarchuk 2006). In any case the high level of band-limited noise ($\sim 27\%$ r.m.s.) we observed is typical of the LHS.

4.2 X/ γ -ray spectral results and constraints

As there is no significant variation in the HR (Fig. 2, right, bottom), we therefore used

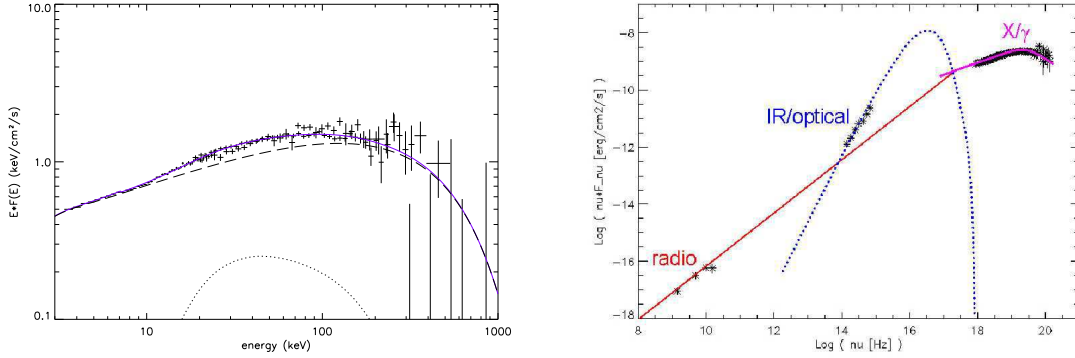


Figure 5: *Left:* $EF(E)$ spectra of SWIFT J1753.5–0127 during our *INTEGRAL* ToO with the PCA, IBIS and SPI data along with the best-fit model (thick): absorbed Comptonization (dashed) convolved by reflection (dotted). *Right:* SED of SWIFT J1753.5–0127 on August 11 with radio, IR, optical and X-ray points (up to 535 keV) and errors. The IR and optical flux densities were dereddened (see CB06b). At least three distinct contributions are seen and interpreted as the optically thick synchrotron emission from a compact jet (red); a thermal disc (blue) and the Comptonization of soft photons by a hot medium (pink).

the whole data from JEM-X, IBIS/ISGRI and SPI of this hard outburst to build up an average spectrum on a wide band together with the simultaneous PCA and HEXTE data. Following the approach described in CB06a when modelling the LHS spectra of Cygnus X-1 and in CB06b, with the `CONS*WABS*(REFLECT*COMPTT)` model (in XSPEC notation), we obtain a reasonable χ^2_{red} of 1.17 (with 121 dof) and $kT_0=0.54^{+0.04}_{-0.07}$ keV, $kT_e=150\pm 26$ keV, $\tau=1.06\pm 0.02$ with $\Omega/2\pi=0.32\pm 0.03$. The relatively high Comptonization temperature can be interpreted as the presence of a medium (corona) which remains hot because of a less important cooling from a reduced number of soft disc photons. The best-fit model over-plotted on the data is reported on Fig. 5 (left) in $EF(E)$ units. The parameters we derive are compatible with the source being in the LHS (e.g., Cadolle Bel et al. 2005, CB06b). The Comptonization parameter $y (= kT_e/m_e c^2 \text{ Max}(\tau, \tau^2))$ is typical of a LHS (~ 0.33) as fully discussed in CB06a for Cygnus X-1.

While our data start at 3 keV, leading to a possible underestimation of the bolometric luminosity, we derive an unabsorbed 2–11 keV flux of 1.5×10^{-9} erg cm $^{-2}$ s $^{-1}$ and a bolometric flux of 1.3×10^{-8} erg cm $^{-2}$ s $^{-1}$. This corresponds to an unabsorbed bolometric luminosity of $5.77 (d/6 \text{ kpc})^2 \times 10^{37}$ erg s $^{-1}$ well below the Eddington regime (even for a low BH mass of $1 M_\odot$). Computing the bolometric luminosity for different distances to SWIFT J1753.5–0127 we derive minimum compact object masses to guarantee that this corresponds to less than 5% of the Eddington luminosity, as seen for BH in the LHS (Maccarone et al. 2003): a $3 M_\odot$ BH implies at least a distance of 4 kpc.

4.3 Optical and radio results

Comparisons of the spectra obtained between July (Torres et al. 2005a, b) and our ToO show the expected behaviour of LMXBs in outburst: bright contribution of a disc in optical followed by a decrease of this contribution simultaneously to a decrease of the soft X-ray flux. We could determine a column density of $(1.97\pm 0.23) \times 10^{21}$ atoms cm $^{-2}$ along the line of sight: this value is consistent with the absorption determined by *Swift*/XRT and it would place the source at ~ 6 kpc (to

be compatible with its absorption and its high latitude value of $l=12.9^\circ$) without requiring intrinsic absorption, with a similar height above the Galactic Plane than those of the LMXB halo sources XTE J1118+480 and Scorpius X-1. Considering the angular resolution of the VLA (the synthesized beam), we detected at all observed frequencies a point-like radio counterpart (angular radius $< 4''$) at a position compatible with the MERLIN one. The radio data are nearly compatible with a flat -or slightly inverted- spectrum since the best-fit leads to $\alpha=-0.17\pm 0.16$ (where $S_\nu \propto \nu^{+\alpha}$).

4.4 Spectral Energy Distribution (SED)

We calculated for radio, IR (with REM-ROSS J, H and K bands thanks to P. D’Avanzo), optical and X-ray data the corresponding flux value in νF_ν units corrected for extinction. The full procedure is described in CB06b. We show in Fig. 5 (right) the SED of SWIFT J1753.5–0127 from radio to X rays in a logarithmic scale. The SED reveals that at least three distinct contributions are necessary: its shape is similar to the ones observed for transient LMXBs (e.g., XTE J1118+480, Chaty et al. 2003; XTE J1720–318, Chaty & Bessolaz 2006).

4.5 Optical and radio constraints

Comparing with nearby faint USNO-B1.0 stars (Monet et al. 2003), we estimate a quiescent visual magnitude above 19.5 mag (from $R > 19.0 \pm 0.5$ and $B > 20.0 \pm 0.5$). Using for example the absolute visual magnitudes from Ruelas-Mayorga (1991), even for the less luminous intermediate type giant companions in the range F8-G2 III, the distance to the source should be ~ 15 kpc, implying a very high minimum BH mass of $\sim 55 M_\odot$ to guarantee $L_{\text{bol}} < 5\% L_{\text{Edd}}$. Clearly, an intrinsically fainter donor is required (a main sequence type K or M companion) rather than earliest types, ranging SWIFT J1753.5–0127 in the LMXB class. Besides, the flat radio spectrum of SWIFT J1753.5–0127 is similar to the ones typically found in BH during LHS (e.g., Fender et al. 2005): it is usually interpreted as synchrotron radiation produced in a partially self-absorbed conical and compact jet (Gallo & Gallo et al. 2003). It is not resolved in our data because it is too faint.

4.6 Discrepancy with the radio/X-ray correlation

Corbel et al. (2003) then Gallo et al. (2003) found a correlation between the X-ray flux and the radio flux density for BH in the LHS (scaled to 1 kpc). We have used our measured unabsorbed X-ray flux to compute the expected radio flux density according to their correlation by using different possible distances to SWIFT J1753.5–0127: the measured value is one order of magnitude lower than the expected one, even for the highest possible distances to the source. This behaviour was already observed for, e.g., XTE J1650–500 (Corbel et al. 2003) and implies that we probably do not constrain very well the k value.

5. Discussion

In these two microquasars, we have observed distinct spectral states and we have determined interesting multiwavelength constraints. Using the broad-band capability of *INTEGRAL*, it has been possible to accumulate a large amount of data on Cygnus X-1 between 5 keV–1 MeV to follow its spectral evolution from 2002 to 2004. We characterized Comptonization parameters changes of the source correlated to the presence of a variable disc emission indicating transitions between the LHS and softer (Intermediate) states. Besides, a high-energy tail during the SIMS emerged from pure Comptonization between 400 keV–1 MeV and was probably associated with a non-thermal component. Also, unusual radio/X-ray correlation was detected.

Besides, we have accurately studied SWIFT J1753.5–0127 over a wide energy band (3 keV–1 MeV). While Comptonization fits well our X/ γ -ray data from *RXTE* and *INTEGRAL* we found that, although clearly in LHS, this source is interestingly well below the radio/X-ray correlation (even assuming a large distance). Another possibility is that SWIFT J1753.5–0127 should radiate more than the Eddington regime but this has never been observed before for a BH in the LHS. The emission could be compatible with the standard picture of synchrotron and inverse Compton radiation coming from a self-absorbed conical jet (Markoff et al. 2005). The extent to which the spectrum hardens at energies approaching 1 MeV has now become an important issue for theoretical modelling of the accretion processes and radiation mechanisms in BH binaries and TS. Such studies will shed light on the accretion processes and radiation mechanisms at work in their vicinity.

References

- [1] Belloni, T. 2005, astro-ph 0507566
- [2] Cadolle Bel, M., Rodriguez, J., Sizun, P., et al. 2004, A&A, 426, 659
- [3] Cadolle Bel, M., Rodriguez, J., Goldwurm, A., et al. 2005, ATEL 574
- [4] Cadolle Bel, M., Sizun, P., Goldwurm, A., et al. 2006a, A&A, 446, 591
- [5] Cadolle Bel, M., Ribó, M., Rodriguez, J., et al. 2006b, submitted to ApJ
- [6] Coppi, P.S., 1999, ASPC, 161, 375
- [7] Chaty, S., Haswell, C. A., Malzac, J., et al. 2003, MNRAS, 346, 689
- [8] Chaty, S. & Bessolaz, N. 2006, accepted for publication in A&A, astro-ph 0605297
- [9] Chen, W., Shrader, C. R. & Livio, M. 1997, ApJ, 491, 312
- [10] Corbel, S., Nowak, M. A., Fender, R. P., et al. 2003, A&A, 400, 1007
- [11] Corbel, S., Fender, R. P., Tomsick, J. A., et al. 2004, ApJ, 617, 1272
- [12] Fender, R. P., Belloni, T. & Gallo, E. 2005, in From X-ray Binaries to Quasars: Black Hole Accretion on All Mass Scales, Eds. T. J. Maccarone, R. P. Fender and L. C. Ho, astro-ph 0506469
- [13] Gallo, E., Fender, R. P., & Pooley, G. G., 2003, MNRAS, 344, 60
- [14] Halpern, J. P. 2005, ATEL 549
- [15] Homan, J., Wijnands, R., van der Klis, M., et al. 2001, ApJS, 132, 377

- [16] Homan, J. & Belloni, T. 2005, *Ap&SS*, 300, 107
- [17] Kalemci, E., 2002, *Bulletin of the American Astronomical Society*, 201, 5705
- [18] Maccarone, T. J. 2003, *A&A*, 409, 697
- [19] Magdziarz, P. & Zdziarski, A. A. 1995, *MNRAS*, 273, 837
- [20] Malzac, J., Petrucci, P.-O., Jourdain, E., et al. 2006, *A&A*, 448, 1125
- [21] Markoff, S., Nowak, M. A. & Wilms, J. 2005, *ApJ*, 635, 1203
- [22] McClintock, J. E. & Remillard, R. A. 2006, in "Compact Stellar X-ray sources" (astro-ph 0306213)
- [23] McConnell, M. L., Zdziarski, A. A., Bennett, K., et al. 2002, *ApJ*, 572, 984
- [24] Miller, J. M., Homan, J. & Miniutti, G. 2006, accepted in *ApJ* (astro-ph 0605190)
- [25] Mitsuda, K., Inoue, H., Koyama, K., et al. 1984, *PASJ*, 36, 741
- [26] Morgan, E., Swank, J., Markwardt, C., et al. 2005, *ATEL* 550
- [27] Morris, D. C., Burrows, D. N., Racusin, J., et al. 2005, *ATEL* 552
- [28] Palmer, D. M., Barthelmey, S. D., Cummings, J. R., et al. 2005, *ATEL* 546
- [29] Rodriguez, J., Corbel, S. & Tomsick, J. A. 2003, *ApJ*, 595, 1032
- [30] Rodriguez, J., Corbel, S., Kalemci, E., et al. 2004, *ApJ*, 612, 1018
- [31] Still, M., Roming, P., Brocksopp, C., et al. 2005, *ATEL* 553
- [32] Stirling, A., Spencer, R. E., de la Force, C. J., et al. 2001, *MNRAS*, 327, 1273
- [33] Tanaka, Y., & Shibazaki, N. 1996, *ARA&A*, 34, 607
- [34] Titarchuk, L.G. 1994, *ApJ*, 434, 570
- [35] Torres, M. A. P., Steeghs, D., Garcia, M. R., et al. 2005a, *ATEL* 551
- [36] Torres, M. A. P., Steeghs, D., Blake, C., et al. 2005b, *ATEL* 566